Developmental Cell
Article

Nucleoporin Levels Regulate Cell Cycle Progression and Phase-Specific Gene Expression

Papia Chakraborty,[1] Yaming Wang,[2] Jen-Hsuan Wei,[1] Jan van Deursen,[3] Hongtao Yu,[4] Liviu Malureanu,[3] Mary Dasso,[5] Douglass J. Forbes,[6] David E. Levy,[2] Joachim Seemann,[1,7] and Beatriz M.A. Fontoura[1,7,*]
[1]Department of Cell Biology, University of Texas Southwestern Medical Center, Dallas, TX 75390, USA
[2]Department of Pathology, New York University School of Medicine, New York, NY 10016, USA
[3]Department of Pediatrics and Adolescent Medicine, Mayo Clinic, Rochester, MN 55905, USA
[4]Department of Pharmacology, University of Texas Southwestern Medical Center, Dallas, TX 75390, USA
[5]Laboratory of Gene Regulation and Development, NICHD, NIH, Bethesda, MD 20892, USA
[6]Section of Cell and Developmental Biology, University of California San Diego, La Jolla, CA 92093, USA
[7]J. Seemann and B.M.A. Fontoura share the senior authorship.
*Correspondence: beatriz.fontoura@utsouthwestern.edu
DOI 10.1016/j.devcel.2008.08.020

SUMMARY

The Nup107-160 complex, the largest subunit of the nuclear pore, is multifunctional. It mediates mRNA export in interphase, and has roles in kinetochore function, spindle assembly, and postmitotic nuclear pore assembly. We report here that the levels of constituents of the Nup107-160 complex are coordinately cell cycle-regulated. At mitosis, however, a member of the complex, Nup96, is preferentially downregulated. This occurs via the ubiquitin-proteasome pathway. When the levels of Nup96 are kept high, a significant delay in G1/S progression occurs. Conversely, in cells of Nup96$^{+/-}$ mice, which express low levels of Nup96, cell cycle progression is accelerated. These lowered levels of Nup96 yield specific defects in nuclear export of certain mRNAs and protein expression, among which are key cell cycle regulators. Thus, Nup96 levels regulate differential gene expression in a phase-specific manner, setting the stage for proper cell cycle progression.

INTRODUCTION

Nuclear transport factors and nuclear pore complex proteins (nucleoporins or Nups) mediate nucleocytoplasmic trafficking in interphase. Both transport factors and certain nucleoporins also have additional functions in mitosis, including spindle assembly and checkpoint functions (Harel and Forbes, 2004; Tran and Wente, 2006). Moreover, nuclear transport is subject to multiple levels of regulation, being impacted by signaling pathways, viral infection, and the proximity of active genes to the nuclear pore complex (NPC) (Tran and Wente, 2006). Furthermore, nucleocytoplasmic transport is specifically regulated during closed mitosis in yeast by molecular rearrangements at the NPC (Makhnevych et al., 2003). These changes in the NPC occur via the interaction of a specific nucleoporin with a transport receptor thus resulting in enhanced cargo release. Since these interactions are specific to mitosis, it underscores the importance of cell cycle in regulating nucleocytoplasmic trafficking and vice-versa (Makhnevych et al., 2003).

Another level of NPC regulation related to the cell cycle is the progressive increase in the number of nuclear pores from G1 to G2, presumably due to a doubling of nucleoporin concentration in preparation for postmitotic nuclear assembly in the daughter cells (Maul et al., 1972, 1980; Winey et al., 1997). Studies performed in a *Xenopus* nuclear reconstitution system demonstrated that the steady increase in nuclear pore numbers can occur by de novo insertion of nucleoporins from both sides of the nuclear envelope to form new nuclear pores (D'Angelo et al., 2006). These observations were made with constituents of the Nup107-160 subcomplex of the NPC, which has a key role in nuclear pore assembly (Harel et al., 2003; Rasala et al., 2006; Walther et al., 2003).

The vertebrate Nup107-160 complex constitutes one third of the proteins of the vertebrate NPC, containing Nup107, Nup160, Nup133, Nup85, Nup96, Sec13, Nup43, Nup37, Seh1, and variably ELYS/MEL-28 (Belgareh et al., 2001; Enninga et al., 2003; Fontoura et al., 1999; Franz et al., 2007; Harel et al., 2003; Loiodice et al., 2004; Orjalo et al., 2006; Rasala et al., 2006; Vasu et al., 2001). Once incorporated into the nuclear pore, the Nup107-160 complex, like its yeast counterpart, the Nup84 complex, plays a key role in mediating mRNA export (Aitchison et al., 1995; Boehmer et al., 2003; Dockendorff et al., 1997; Emtage et al., 1997; Faria et al., 2006; Teixeira et al., 1997). In mitosis, the Nup107-160 complex assumes other important functions, being incorporated into both kinetochores and the centrosomes/proximal spindle poles (Enninga et al., 2003; Loiodice et al., 2004; Orjalo et al., 2006; Rasala et al., 2006). Indeed, depletion of the Nup107-160 complex disrupts the correct formation of spindle microtubules in mitotic *Xenopus* egg extracts (Orjalo et al., 2006) and compromises kinetochore function (Zuccolo et al., 2007). Here we report that the Nup107-160 complex is cell cycle-regulated. In particular, Nup96 is preferentially downregulated in mitosis via the ubiquitin-proteasome pathway. We show that this regulation of Nup96 controls cell cycle progression and differential phase-specific gene expression of key cell cycle regulators.

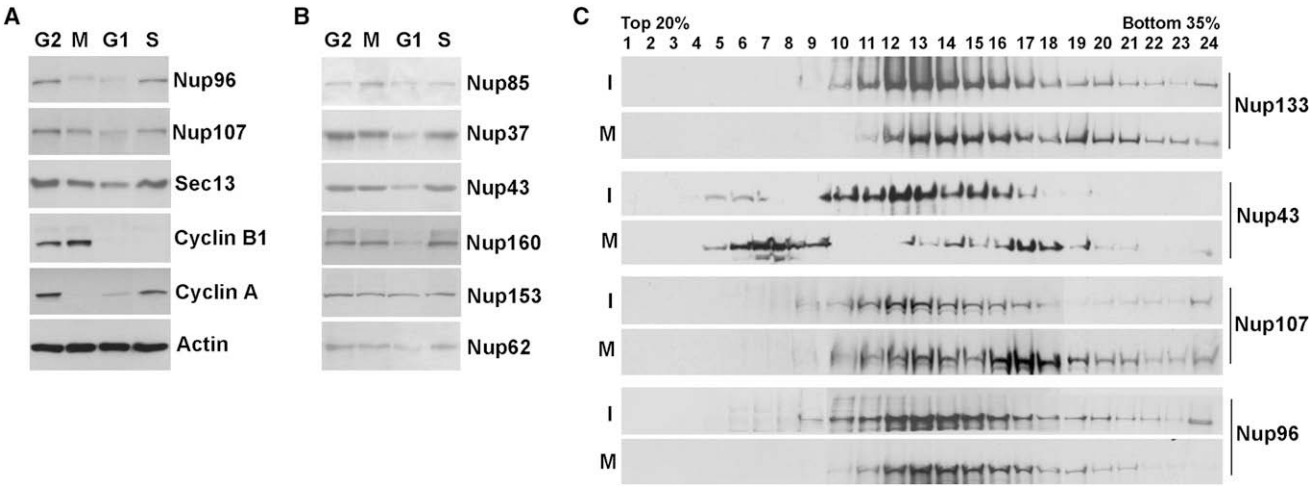

Figure 1. Nucleoporins Are Regulated throughout the Cell Cycle

(A and B) Immunoblot analysis was performed on HeLa cell lysates synchronized at different phases of the cell cycle with antibodies against the depicted proteins (n = 8).

(C) Interphase and mitotic lysates of HeLa cells were loaded onto a 20%–35% sucrose gradient. Samples were analyzed by SDS-PAGE with the indicated antibodies.

RESULTS

Expression of the Nup107-160 Complex Is Cell Cycle Regulated

To ask whether the constituents of the Nup107-160 complex are differentially regulated in a cell cycle-dependent manner, we synchronized HeLa cells and performed immunoblot analysis on cell extracts obtained from different phases of the cell cycle. We found that the levels of Nup107, Sec13, Nup85, Nup37, Nup43, Nup160, Nup153, and Nup62 increased from G1 to G2/M phases of the cell cycle (Figures 1A and 1B), as would be predicted from the electron microscopic visualization of nuclear pore doubling that occurs at S phase (Maul et al., 1972, 1980; Winey et al., 1997). Notably, the level of Nup96, a member of the Nup107-160 complex, although increasing from G1 to G2, was preferentially downregulated 50%–60% in early mitosis (Figure 1A). This level of change was not seen for the other nucleoporins at mitosis. Cyclins A and B served as controls. Cyclin A was downregulated in early mitosis, as expected, while cyclin B was upregulated in early mitosis and degraded in anaphase (Figure 1A; Murray, 2004). Upon further analysis, sucrose gradient sedimentation of interphase and mitotic extracts of HeLa cells revealed that a very significant pool of Nup43 is partially dissociated from the Nup107-160 complex at mitosis, indicating that the Nup107-160 complex is not identical in interphase and mitosis (Figure 1C).

Nup96 Is Downregulated in Mitosis via the Proteasome

Since Nup96 levels were downregulated in mitosis, we set out to determine the mechanism involved in this process. We first confirmed the observed reduction in Nup96 levels in early mitosis using multiple methods of cell synchronization. HeLa cells were synchronized at the G1/S border with a double thymidine block, followed by treatment with nocodazole, taxol, or colcimid to block cells in mitosis. All three sets of mitotic cells showed a decrease in Nup96 protein levels compared to control asynchronous cells (Figures 1A and 2A). We observed a similar reduction in Nup96 levels in HeLa cells after mitotic cell shake-off, which was performed to exclude any potential effect of particular drugs on the expression levels of Nup96 in mitosis (Figure 2B). The decrease in Nup96 levels at mitosis was also observed in other cell types, such as primary mouse embryo fibroblasts (MEF) (Figure 2C) and human 293T cells (data not shown). Furthermore, we found that this mitotic downregulation of Nup96 does not occur at the mRNA level (Figure 2D). Quantification of Nup96 mRNA levels between the G2 and M phases, by real-time PCR, did not show significant differences (Figure 2D).

We next asked whether downregulation of Nup96 in mitosis involved proteasome-mediated degradation. HeLa cells were treated with nocodazole in the presence or absence of the proteasome inhibitor lactacystin and the levels of Nup96 in mitosis were analyzed by immunoblot. In the presence of lactacystin, the Nup96 level in mitosis was higher than in the absence of lactacystin (Figure 2E). This result indicated that Nup96 is a substrate of the proteasome. In contrast, the levels of Nup160 or actin did not change to the same extent as Nup96 in the presence of lactacystin (Figure 2E). To further investigate whether Nup96 degradation occurs via the ubiquitin pathway, we transfected 293T cells with plasmids encoding HA-tagged ubiquitin alone (Figure 2F) or myc-tagged Nup96 in combination with HA-tagged ubiquitin (Figures 2G; see Figure S1A and Supplemental Data available online), and performed immunoprecipitation using anti-Nup96 antibodies or anti-HA antibody. Overexpression of HA-ubiquitin should compete with endogenous ubiquitin and become covalently conjugated to target proteins. We were able to immunoprecipitate HA-tagged ubiquitinated forms of endogenous Nup96 (Figure 2F, lanes 3 and 4) or overexpressed Nup96 (Figure 2G and Figure S1A). Moreover, ladders of polyubiquitin conjugates of Nup96 were enriched in the presence of the proteasome inhibitor MG132 (Figure S1A). Thus, both endogenous and ectopically expressed Nup96 are ubiquitinated in vivo.

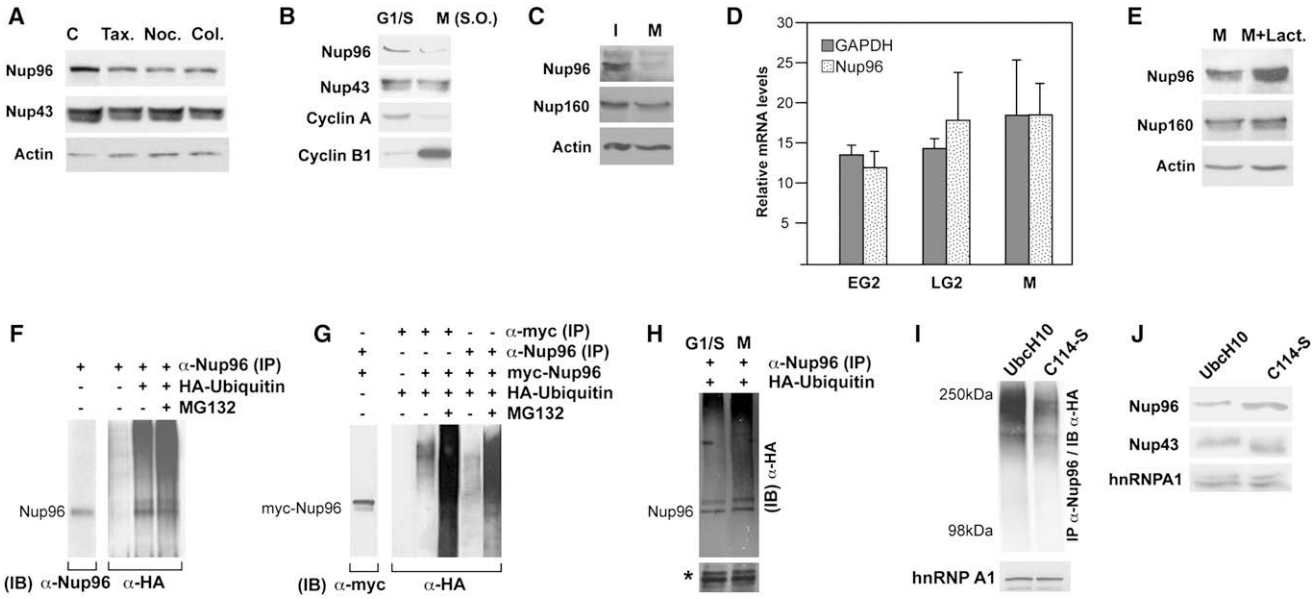

Figure 2. Nup96 Is Downregulated in Mitosis via the Ubiquitin-Proteasome Pathway

(A) HeLa cells were treated with thymidine followed by nocodazole, colcemid, or taxol, and immunoblot analysis was performed with anti-Nup96, anti-Nup43, or anti-actin antibodies. C, control showing Nup96 levels in asynchronous cell extract.

(B) Mitotic HeLa cells obtained by the shake-off procedure were subjected to immunoblot analysis with antibodies against Nup96, Nup43, Cyclin A, and Cyclin B1.

(C) Asynchronous and mitotic MEF lysates were subjected to immunoblot analysis with anti-Nup96, anti-Nup160, or anti-actin antibodies.

(D) RNA was isolated from HeLa cells synchronized at early G2 (EG2), late G2 (LG2), and M phases of the cell cycle. Nup96 and GAPDH mRNA levels were quantified by real time RT-PCR. Results are the mean ± SD.

(E) Mitotic cells were untreated or treated with lactacystin and cell extracts were subjected to immunoblot analysis with antibodies against Nup96, Nup160, and actin.

(F) 293T cells were transfected with a plasmid encoding HA-Ubiquitin, and MG132 was added for 12 hr. Cell extracts were subjected to immunoprecipitations followed by immunoblot analysis with the depicted antibodies. IP, immunoprecipitation; IB, immunoblot.

(G) 293T cells were transfected with plasmids encoding myc-Nup96 or HA-Ubiquitin alone or cotransfected with myc-Nup96 and HA-Ubiquitin. Cell extracts were subjected to immunoprecipitation and immunoblot analysis with the depicted antibodies.

(H) 293T cells expressing HA-ubiquitin were synchronized at the G1/S border or at mitosis. Cell extracts were subjected to immunoprecipitation with anti-Nup96 antibodies followed by immunoblot analysis with anti-HA antibody. Asterisk shows equal sample input.

(I) 293T cells were cotransfected with HA-Ubiquitin and UbcH10, or C114-S. Cells were incubated with MG132 for 12 hr and cell extracts were immunoprecipitated with anti-Nup96 antibodies followed by immunoblot analysis with anti-HA antibody. hnRNP A1 was used as loading control.

(J) HeLa Tet–On cells were transfected with plasmids encoding UbcH10 or C114-S. Cell extracts were subjected to immunoblot analysis with antibodies against Nup96, Nup43, or hnRNPA1. Nup96 levels increased 3.5-fold in the presence of the transfected dominant negative mutant of UbcH10 (C114-S).

To determine whether ubiquitination of Nup96 is increased in mitosis, cells were transfected with HA-ubiquitin for 24 hr. Then, the transfected cells were incubated with thymidine for 14 hr to obtain cell cultures enriched at the G1/S border, or incubated with nocodazole for 14 hr to collect cells in mitosis. Cell extracts were subjected to immunoprecipitation with anti-Nup96 antibodies followed by immunoblot analysis with anti-HA antibody. Indeed, increased ubiquitination of Nup96 was observed in mitosis, as compared to cells at the G1/S border (Figure 2H). This increase in Nup96 ubiquitination supports the findings showing downregulation of Nup96 in mitosis at the protein level. We also observed that other Nups, such as Nup107 (Figure S1B) and Sec13 (data not shown), can be ubiquitinated, though their levels do not change significantly in mitosis as in the case of Nup96. These observations indicate that ubiquitin-mediated proteolysis is a mechanism involved in nucleoporin turnover. However, in the case of Nup96, ubiquitination and proteasome-mediated degradation are enhanced in mitosis, which is the mechanism by which Nup96 is preferentially downregulated.

To further analyze the proteolysis of Nup96 in mitosis, we carried out experiments with the mitosis-specific ubiquitin-conjugating enzyme UbcH10 to determine if it has a role in the mitotic degradation of Nup96. UbcH10 is known to be involved in mediating degradation of mitotic-specific substrates such as cyclin A and cyclin B (Peters, 2002). To test whether inhibition of UbcH10 activity in mitosis would diminish Nup96 proteolysis, cotransfection experiments in HeLa cells were performed with plasmids encoding myc-tagged Nup96 and either wild-type UbcH10 or a dominant-negative mutant form of UbcH10, C114-S. UbcH10 (C114-S) inhibits both cyclin A and B degradation, as well as the metaphase to anaphase transition (Townsley et al., 1997). Indeed, overexpression of the C114-S mutant of the mitosis-specific ubiquitin-conjugating enzyme UbcH10 inhibited both Nup96 ubiquitination (Figure 2I) and Nup96 degradation (Figure 2J). On the other hand, C114-S did not significantly affect the levels of Nup43 or hnRNPA1 (Figure 2J). Since UbcH10 is a mitosis-specific E2 enzyme, these results indicate that Nup96 is ubiquitinated and also preferentially degraded in mitosis.

Table 1. High Levels of Nup96 in Mitosis Slightly Alter Mitotic Timing

Cells	Transfectant	NEB-Metaphase	Metaphase-Anaphase	Anaphase-Cytokinesis
HeLa Tet-On	+ control plasmid	34 (±6)	21 (±4)	10 (±2)
n = 23	+ FLAG-Nup96	30 (±4)	29 (±4)*	13 (±2)*
HeLa Tet-On	+ EGFP	29 (±8)	19 (±7)	10 (±1)
n = 28	+ EGFP-Nup37	26 (±6)	19 (±8)	12 (±3)
NRK	+ EGFP	21 (±5)	14 (±7)	10 (±1)
n = 14	+ myc-Nup96	18 (±4)*	12 (±6)	7 (±3)*

Tet-On HeLa cells were stably transfected with plasmid alone (control) or plasmid encoding FLAG-Nup96, and Nup96 expression was induced by doxycyclin (n = 23). Tet-On HeLa cells were also transfected with plasmids encoding EGFP (control) or EGFP-Nup37 (n = 28). NRK cells were transfected with myc-Nup96 and EGFP (5:1) or, as control, transfected with EGFP and vector alone (5:1) (n = 14). Mitotic chromosomes labeled with H2B-YFP were followed over time by fluorescence and phase contrast. Time zero was marked by the nuclear envelope breakdown (NEB). *$p < 0.05$. Results are the mean ± SD.

Nup96 Levels Regulate Cell Cycle Progression

To determine the functional significance of Nup96 downregulation in mitosis, we investigated whether Nup96, if present at high levels, has effects on mitotic timing. We generated stably transfected HeLa cell lines expressing high levels of FLAG-tagged-Nup96 (data not shown) and coexpressed histone H2B-YFP to follow live cells as they transitioned through mitosis. In the presence of excess Nup96, we observed a slight delay from metaphase to anaphase and from anaphase to cytokinesis (Table 1). These modest effects of high levels of Nup96 on mitotic timing did not result in any major mitotic defect. We also followed mitotic progression in the presence of high levels of Nup37, another constituent of the Nup107-160 complex, and again did not detect any major effect on mitotic timing or mitotic defects (Table 1). In addition, we tested whether high levels of Nup96 would affect mitotic timing of normal rat kidney (NRK) cells, which have an intact G1 checkpoint. We show, in Table 1, that increased levels of Nup96 had modest effects on mitotic timing in NRK cells causing a slight acceleration from NEBD to metaphase and from anaphase to cytokinesis. Although these minor defects on mitotic timing caused by high levels of Nup96 varied between HeLa cells and NRK cells (Table 1), in both cases they did not result in any major mitotic defect.

However, we observed that high levels of Nup96 resulted in a prominent delay in G1/S progression. In this experiment we also used NRK cells because they have an intact G1 checkpoint. NRK cells were synchronized in S phase with aphidicolin, then transfected 3 hr after release from aphidicolin with plasmids encoding Nup96, Nup37, ALADIN, or EGFP, at a time when the cells were in late G2. Under these conditions, detectable protein expression occurs in G1, after plasmids efficiently enter the nucleus following nuclear envelope breakdown in mitosis. BrdU staining was performed 19 hr after the aphidicolin release and cells were analyzed by immunofluorescence and Apotome microscopy (Figure 3A). Quantification of BrdU-positive cells, indicative of cells having entered S phase, was carried out. The data showed that approximately half of the population of cells expressing high levels of Nup96 was still in G1 at 19 hr (Figure 3A), while the majority of cells expressing high levels of the control EGFP protein had already progressed into S phase, which was set to 100% (Figure 3A). High expression levels of the nucleoporins Nup37 or ALADIN did not result in any inhibition of G1 progression. In fact, high levels of ALADIN showed an acceleration of G1 progression. Thus, we conclude that high levels of Nup96 delay G1 progression or impede the G1/S transition.

To further examine the significance of regulating Nup96 levels in vivo, we used our Nup96$^{+/-}$ mouse model, where cells express low levels of Nup96 (Faria et al., 2006). We had a previous indication that T cells derived from Nup96$^{+/-}$ mice proliferated faster than those from Nup96$^{+/+}$ mice, as assessed by thymidine incorporation (Faria et al., 2006). However, the mechanisms underlying this proliferation defect have not been investigated. Here we report, using different methods to assess cell proliferation, that both T cells and bone marrow-derived macrophages (BMDM) from Nup96$^{+/-}$ mice show an acceleration of the cell cycle, with this phenotype being most pronounced in T cells. This was observed after resting T cells (G0 phase), obtained from spleen, were labeled with CSFE and induced to proliferate with anti-CD3 and anti-CD28 antibodies. CSFE, a fluorescent dye, binds covalently to cytoplasmic proteins. Following each cell division, the fluorescence intensity of CSFE is reduced, which is quantified by flow cytometry. Nup96$^{+/-}$ T cells showed a higher reduction in fluorescence intensity between day 1 and day 2 than Nup96$^{+/+}$ T cells, indicating that Nup96 mutant cells proliferated faster than wild-type cells (Figure 3B). Similar results were obtained when T cells from the spleen, mesenteric lymph nodes (MLN), and peripheral lymph nodes (PLN) of Nup96$^{+/+}$ and Nup96$^{+/-}$ mice were induced to proliferate with anti-CD3 and anti-CD28 antibodies for 72 hr, and their proliferation was measured by thymidine incorporation. Lastly, we examined growth rates of bone marrow-derived macrophages (BMDM) from Nup96$^{+/+}$ and Nup96$^{+/-}$ mice. An equal number of cells was incubated with IL-3 conditioned and MEF-conditioned medium. The number of BMDM cells was then calculated after 48 hr by measuring the activity of the mitochondrial reductase enzymes, which correlates to cell number. Proliferation of BMDM was slightly enhanced in Nup96$^{+/-}$ cells as compared to Nup96$^{+/+}$ cells (Figure 3B). Cell cycle acceleration was, notably, more prominent in T cells than in macrophages, especially in the case of T cells obtained from mesenteric lymph nodes (Figure 3B; Faria et al., 2006).

Nup96 Levels Regulate Expression of Key Cell Cycle Regulators

One explanation for the observed effect on cell proliferation might be that inappropriate levels of Nup96 in G1 may interfere with certain key aspects of gene expression related to cell cycle progression. Thus, mRNA abundance, nucleocytoplasmic distribution of mRNAs, and protein expression of key cell cycle regulators were assessed in G1. To test for such effects using a physiological model, we obtained resting T cells (G0) from the spleens of Nup96$^{+/+}$ or Nup96$^{+/-}$ mice. These cells were then stimulated for 2 hr with anti-CD3 and anti-CD28 antibodies to enter G1. As expected, both Nup96$^{+/+}$ and Nup96$^{+/-}$ T cells similarly transitioned into G1 after 2 hr stimulation, as demonstrated by the comparable fold-induction of IκBα mRNA levels in both cell types (Figure 4A). Increase in IκBα mRNA levels

A

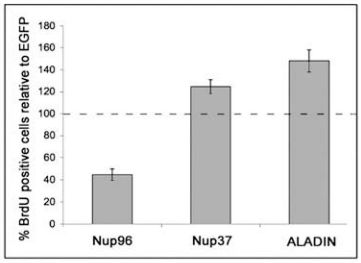

B

ΔCSFE Fluorescence Intensity	Nup96+/+	Nup96+/-
Spleen T cells	75 ± 10	122 ± 20*
Thymidine Incorporation CPM X10⁴		
Spleen T cells	20 ± 2	56 ± 10.2*δ
MLN T cells	9 ± 0.1	34 ± 5*δ
PLN T cells	50 ± 0.1	91 ± 9.8*δ
MTT Assay % increase in cell number		
BMDM	0	21 ± 0.6*

δ , (Faria *et al*, 2006)
*p < 0.05

Figure 3. Abnormal Levels of Nup96 Alter Cell Cycle Progression

(A) NRK cells synchronized in S phase with aphidicolin were transfected in G2 with plasmids encoding EGFP, myc-Nup96, EGFP-Nup37, or EGFP-ALADIN. Cells were labeled with BrdU and subjected to immunofluorescence with anti-BrdU and anti-myc antibodies or anti-GFP antibodies. Cells in S phase (BrdU-positive cells) were scored by microscopy. Dashed line represents control cells transfected with EGFP alone.

(B) T cells, obtained from Nup96$^{+/+}$ and Nup96$^{+/-}$ mice, were labeled with CSFE and proliferation was induced by addition of anti-CD3 and anti-CD28 antibodies. CSFE fluorescence intensity was measured by flow cytometry at days 1 and 2. The difference in median fluorescence intensity of samples obtained at days 1 and 2 are shown (Δ CSFE). Proliferation of T cells from spleen, mesenteric lymph modes (MLN), or peripheral lymph nodes (PLN) stimulated with anti-CD3 and anti-CD28 antibodies for 72 hr was measured by thymidine incorporation as we reported (Faria et al., 2006). BMDM were induced to proliferate with 10% WEHI medium and 20% MEF conditioned medium. Proliferation was assessed on days 2, 3, and 4 using the CellTiter 96® Non-Radioactive Cell Proliferation Assay.

correlates with entry into G1 as NFκB is imported into the nucleus and activates the transcription of the IκBα gene as part of a feedback mechanism (Hoffmann et al., 2002). Since mouse T cells, when stimulated, complete one cell cycle within ~5–6 hr (van Stipdonk et al., 2001), we labeled stimulated T cells with the DNA dye propidium iodide at 2 hr and determined whether the cells had progressed into S/G2. As shown in Figures 4B and 4C, T cells from Nup96$^{+/+}$ and Nup96$^{+/-}$ mice did not progress into S or G2 after 2 hr of stimulation with anti-CD3 and anti-CD28 antibodies.

The G1 T cell population of Nup96$^{+/-}$ mice was then examined for potential defects in gene expression. We found that the low levels of Nup96 in Nup96$^{+/-}$ T cells did not cause significant changes in the levels of various mRNAs including those that encode key cell cycle regulators, such as Cyclin D3 and CDK6, but downregulated IκBα mRNA levels (Figure 4D). However, the nuclear/cytoplasmic distribution (N/C ratio) of mRNAs in Nup96$^{+/-}$ T cells was affected. The mRNAs that encode the G1 cell cycle regulators, Cyclin D3, CDK6, and IκBα, were more prevalent in the cytoplasm of Nup96$^{+/-}$ T cells than in Nup96$^{+/+}$ T cells in G1. In contrast, the distribution of Eβ mRNA, an immune-related gene, was more predominant in the nucleus (Figure 4E). The nuclear/cytoplasmic ratio of GAPDH, ICAM-1, or α-tubulin mRNAs did not change in the presence of low levels of Nup96 (Figure 4E). At the protein level, immunoblot analysis performed as cells entered G1 (2 hr time point) showed that Cyclin D3 level was ~3-fold higher in Nup96$^{+/-}$ cells than in Nup96$^{+/+}$ cells, while CDK6 protein was lower. The protein levels of β-actin and IκBα did not change between Nup96$^{+/+}$ and Nup96$^{+/-}$ T cells (Figure 4F). By 28 hr, cells had undergone several cycles in which the heterozygous T cells had proliferated faster than wild-type cells. While cells were not in synchrony at this time point, it was clear that CDK6 protein levels significantly increased (~8-fold) in Nup96$^{+/-}$ cells as compared to other proteins analyzed in both Nup96 mutant and wild-type T cells. The specific dynamics of protein synthesis and turnover may obscure some effects (such as on IκBα, compare Figures 4D and 4F), but overall we conclude that Nup96 dosage controls expression of key cell cycle regulators, such as Cyclin D3 and CDK6. The abnormalities in gene expression detected in the first cycle due to low levels of Nup96 likely accumulated over time, yielding defects in cell proliferation.

mRNA Distribution Is Cell Cycle-Dependent

The cell cycle-dependent regulation of Nup96 and its role in differentially regulating gene expression in G1 prompted us to investigate whether the levels and distribution of mRNAs vary between different phases of the cell cycle. Indeed, we found that bulk mRNA levels are ~85% higher in G2 cells than in G1 cells, as determined by oligo-dT in situ hybridization and flow cytometry (Figure 5A). Furthermore, the nuclear/cytoplasmic (N/C) distribution of poly(A) RNA, measured by fluorescence intensity, showed that G2 cells presented a lower N/C ratio of poly(A) RNA than G1 cells (Figures 5B and 5C). These results indicate that, in the G2 phase, mRNA export may be enhanced.

These findings were further corroborated by in situ hybridization using probes that recognize specific mRNAs. Immunofluorescence with anti-Cyclin B1 antibody was performed simultaneously to identify cells in G2. As shown in Figure 5D, nucleocytoplasmic distribution of specific mRNAs varied depending on the phase of the cell cycle. β2-microglobulin, α-tubulin, and Cyclin B1 mRNAs were more prevalent in the cytoplasm in G2 cells than in G1 cells. We also observed a similar increase in cytoplasmic localization of β2-microglobulin and α-tubulin mRNAs in MEF by real-time PCR (Figure S2A). In macrophages, Cyclin B1, IkBα, and ICAM-1 mRNAs were also predominantly more cytoplasmic in G2 than in G1 (Figure S2B), showing a similar nucleocytoplasmic mRNA distribution as in MEF and HeLa cells. However, the nucleocytoplasmic distribution of the RPS11 mRNA, in macrophages, was unaltered between G1 and G2 (Figure S2B). Taken together, these results indicate that the intracellular distribution of bulk mRNA is differentially regulated in a cell cycle-dependent manner, between G1 and G2, with a significant increase in cytoplasmic mRNA in G2.

We next quantified the abundance and nucleocytoplasmic distribution of various mRNAs in G1 and G2 cells to ask whether the regulation of Nup96 levels is key to maintaining the fine balance of mRNA distribution during the cell cycle. BMDM were

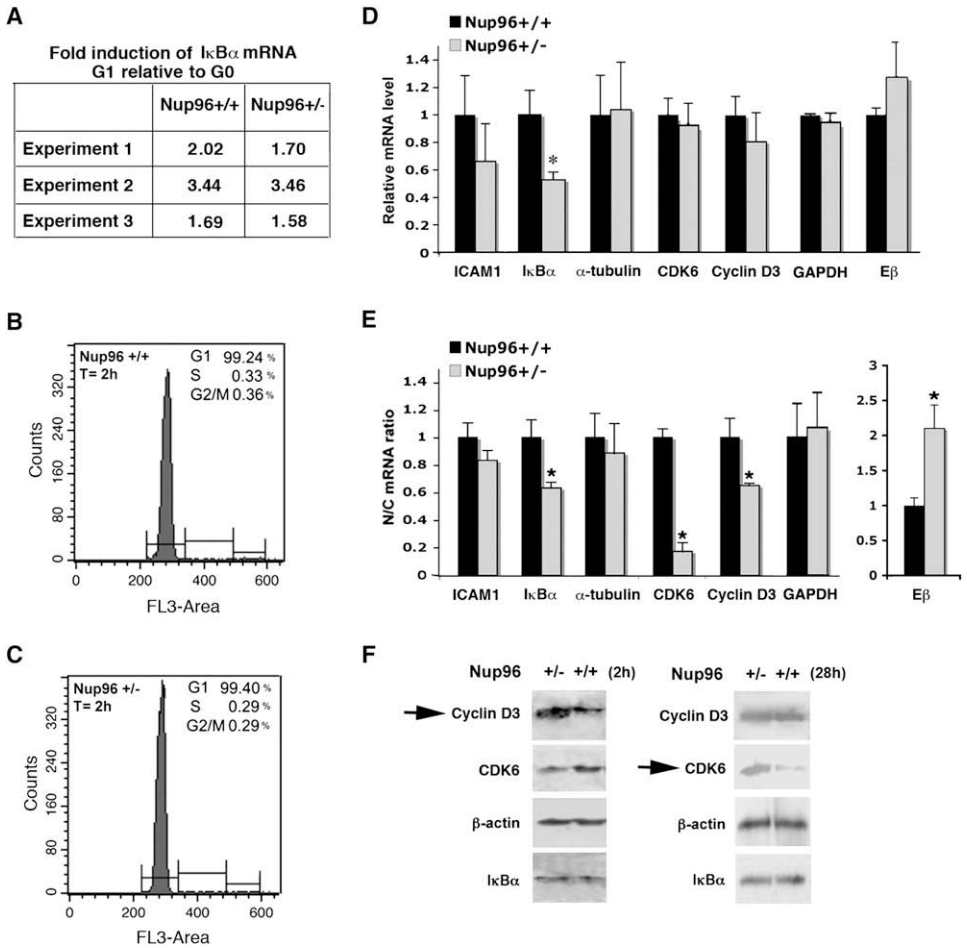

Figure 4. Nup96 Differentially Regulates Expression of Key Cell Cycle Regulators

(A) T cells from Nup96$^{+/+}$ and Nup96$^{+/-}$ mice were isolated from spleen (G0) and then incubated for 2 hr with anti-CD3 and anti-CD28 antibodies to enter G1. RNA was isolated and RT-PCR was performed to quantify IκBα mRNA levels in samples from three different mice of each genotype (n = 3).

(B and C) Cell cycle analysis of proliferating T cells. Resting T cells were incubated for 2 hr with anti-CD3 and anti-CD28 antibodies and DNA was stained with propidium iodide. Cells were analyzed by flow cytometry.

(D) RNA was isolated from total T cell extracts of Nup96$^{+/+}$ and Nup96$^{+/-}$ mice after 2 hr of stimulation with anti-CD3 and anti-CD28 antibodies. mRNA levels of various mRNA species were then quantified by RT-PCR. Samples were normalized against the following housekeeping genes' mRNAs: β-actin, RPS11, L32, and GAPDH. Results are the mean ± SD (n = 3).

(E) RNA was isolated from nuclear and cytoplasmic fractions of T cells from Nup96$^{+/+}$ and Nup96$^{+/-}$ mice after 2 hr of stimulation with anti-CD3 and anti-CD28 antibodies. mRNA levels of various mRNA species were quantified as in (D). Results are the mean ± SD (n = 3). N/C, nuclear/cytoplasmic mRNA ratio. *$p < 0.05$.

(F) Resting T cells were incubated for 2 hr (n = 2) or 28 hr (n = 3) with anti-CD3 and anti-CD28 antibodies. Cell extracts were subjected to immunoblot analysis with the depicted antibodies. Arrows show the increase in Cyclin D3 and CDK6 levels in the Nup96$^{+/-}$ T cells.

stimulated to proliferate with macrophage colony-stimulating factor (M-CSF). Growth stimulation with M-CSF alone did not induce abnormal proliferation of Nup96$^{+/-}$ BMDM (Figure 6A). However, as shown in Figure 3B, enhanced proliferation of Nup96$^{+/-}$ BMDM was observed in the presence of IL-3 conditioned and MEF-conditioned medium, which contain multiple growth factors and hence provide a stronger growth stimulus than M-CSF alone. Thus, RNA was isolated from total cell extracts and from nuclear and cytoplasmic fractions of Nup96$^{+/+}$ or Nup96$^{+/-}$ BMDM that were stimulated with M-CSF alone to obtain synchronous samples, in G1 and G2. The abundance of various mRNA species was then quantified by real-time PCR. The expected upregulation of Cyclin B1 and α-tubulin mRNAs from G1 to G2 in both Nup96$^{+/+}$ and Nup96$^{+/-}$ macrophages further demonstrated the synchronous cell cycle progression upon M-CSF treatment and served as control for both phases (Figure 6B; Whitfield et al., 2002). We observed that the total abundance of various mRNAs tested was not significantly altered in the presence of low levels of Nup96, including that of key cell cycle regulators such as Cyclin B1 and Cyclin D3 (Figure 6C). In contrast, the nuclear/cytoplasmic ratios of certain mRNAs were differentially regulated in G1 and G2. In G2, as opposed to G1, the mRNAs encoding Cyclin D3, L32, and ICAM-1 were preferentially localized to the nucleus of Nup96 mutant cells as compared to Nup96$^{+/+}$ cells (Figure 6D). In contrast, the nuclear/cytoplasmic distribution of RPS11, α-tubulin, and Cyclin

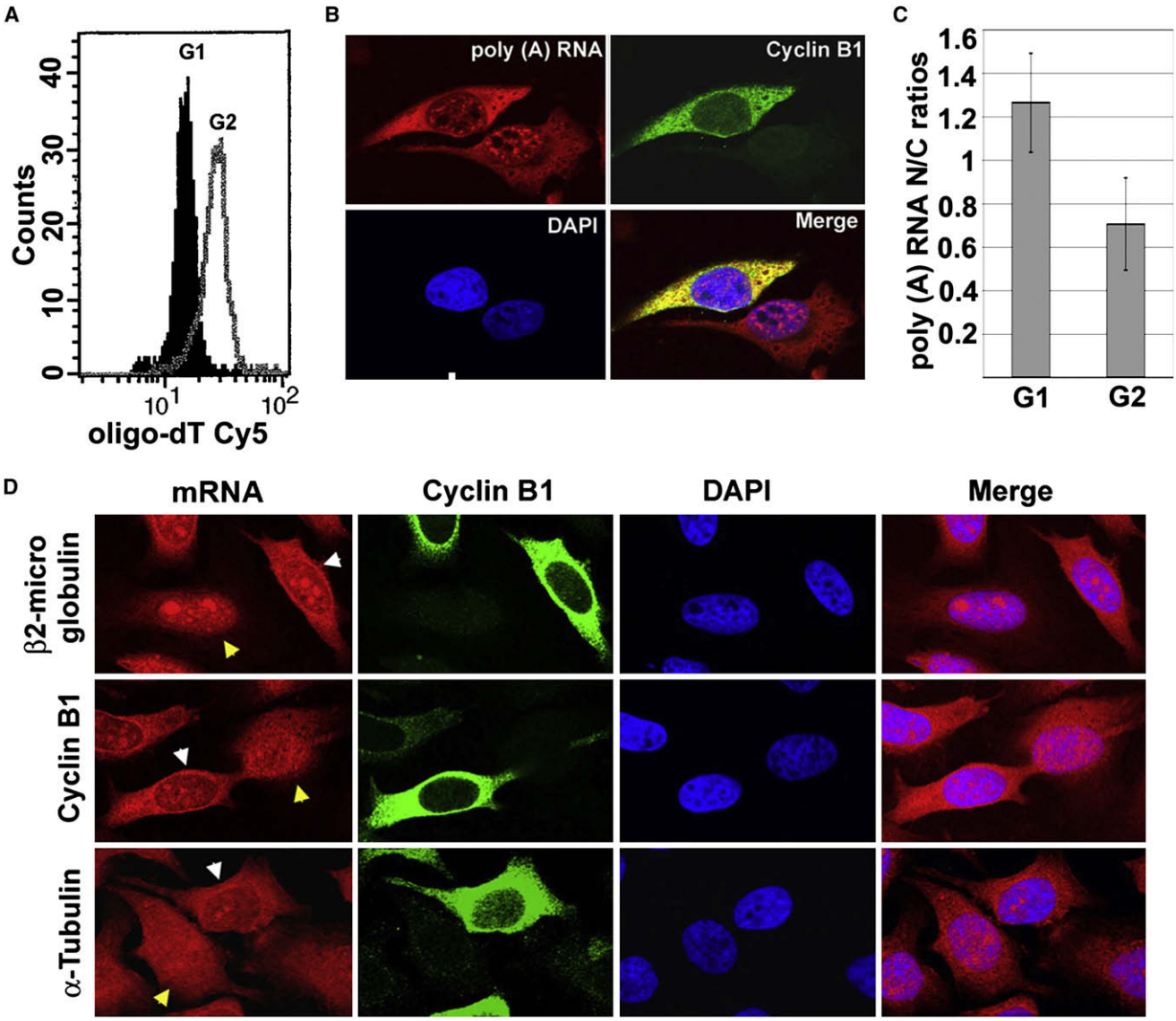

Figure 5. Differential Regulation of mRNA Export between the G1 and G2 Phases of the Cell Cycle

(A) Quantification of bulk poly(A) RNA from HeLa cells in G1 and G2. Bulk poly(A) RNA was stained with a biotinylated oligo-dT probe and counterstained with PI. Biotinylated oligo-dT was detected with Cy5-streptavidine and quantification was performed by flow cytometry.

(B) Intracellular distribution of bulk poly(A) RNA in G1 and G2. Bulk poly(A) RNA was visualized in cells by oligo-dT in situ hybridization. Immunofluorescence was simultaneously performed with anti-Cyclin B1 antibody to detect cells in G2. Samples were analyzed by Apotome microscopy.

(C) Mean nuclear and cytoplasmic intensities were analyzed using the Axiovision 4.0 software and the nuclear/cytoplasmic (N/C) ratios were calculated.

(D) In situ hybridization was performed with specific probes for the depicted mRNAs and samples were processed and analyzed as in (B). White arrows denote cells in G2, while yellow arrows show cells in G1 or early S. The decrease in mean N/C ratios of the β2-microglubulin, Cyclin B1, and α-tubulin mRNAs, from G1 to G2, was similar (~1.42 in G1 to 0.79 in G2, with a $p < 0.009$).

B1 mRNAs did not significantly change between G1 and G2 in Nup96$^{+/-}$ cells relative to Nup96$^{+/+}$ cells (Figure 6D).

Altogether, the results show that: (1) bulk mRNA export is cell cycle regulated, (2) Nup96 plays a role in differentially regulating nucleocytoplasmic distribution and expression of certain mRNAs in a cell cycle-dependent manner, and (3) among the Nup96-regulated mRNAs and proteins are key cell cycle regulators. We have also shown that the pattern of this regulation is cell-type specific.

DISCUSSION

We report here the regulation of nucleoporin levels of key constituents of the Nup107-160 complex throughout the cell cycle and its functional significance. The progressive increase in levels of the Nup107-160 complex from G1 to G2 accompanies the known doubling in NPC number which occurs within this time frame (Maul et al., 1972), as well as the increase in bulk poly(A) RNA shown here. Other nucleoporins, such as Nup153, were

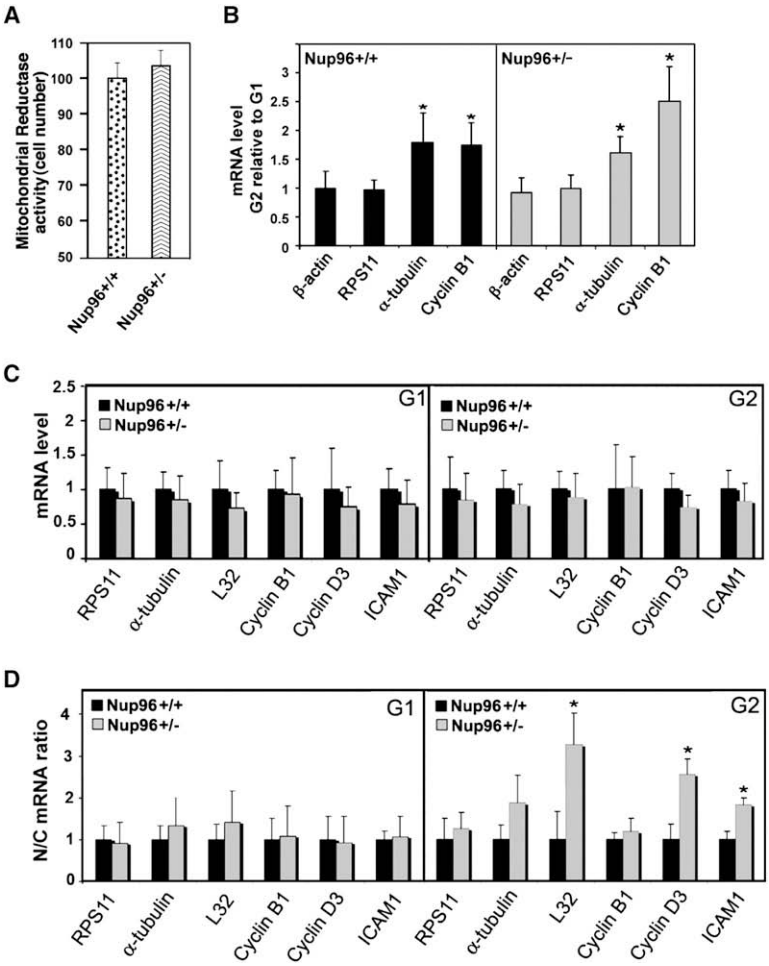

Figure 6. Nup96 Levels Regulate Nucleocytoplasmic Distribution of Certain mRNAs in G1 and G2

(A) Mitochondrial reductase enzyme activity was measured to access cell proliferation of BMDM from Nup96$^{+/+}$ and Nup96$^{+/-}$ mice cultured in the presence of M-CSF. A normalized value of the absorbance of samples at 560 nm is plotted with the wild-type values set to 100%.

(B–D) BMDM isolated from Nup96$^{+/+}$ or Nup96$^{+/-}$ mice were synchronized and harvested during G1 or G2. The levels of various mRNAs species were measured by RT-PCR using gene-specific primers, and were normalized against GAPDH mRNA levels. Results are the mean ± SD (n = 3). *p < 0.05. Nup96$^{+/+}$ values are set to 1.

(B and C) Total mRNA levels were compared as cells progressed from G1 to G2.

(D) Nuclear (N) to cytoplasmic (C) ratios of each transcript were also obtained and compared.

not upregulated to the same extent from G1 to G2 as the Nup107-160 complex. In mitosis, we observed additional changes in the composition of the Nup107-160 complex. Nup96 was preferentially downregulated in mitosis, while Nup43 was partially displaced from the complex. These results indicate that nucleocyoplasmic transport and/or composition of the NPC varies in a cell cycle-dependent manner.

Since both the Nup107-160 complex and Nup153 are involved in mRNA export (Ball et al., 2007; Boehmer et al., 2004; Faria et al., 2006), the difference in levels of these nucleoporins throughout the cell cycle implied that differential mRNA export might occur between the G1 and G2 phases of the cell cycle. Indeed, we show that the nucleocytoplasmic distribution of certain mRNAs and protein expression are differentially regulated between G1 and G2 in a cell-type specific manner, and that Nup96, a constituent of the Nup107-160 complex, has a key role in this mechanism. Low levels of Nup96 in T cells resulted in an enhanced cytoplasmic localization of cyclin D3, which paralleled an increase in protein expression in the first G1 cycle, 2 hr after the proliferation stimuli had been applied. CDK6 protein level was lower at 2 hr in Nup96$^{+/-}$ cells than in Nup96$^{+/+}$ cells, while the cytoplasmic localization of its mRNA was enhanced. However, the Nup96 mutant cells showed high levels of CDK6 protein 28 hr after the induction of proliferation. Both Cyclin D3 and CDK6 are known to drive cell cycle progression (Murray, 2004). High levels of Cyclin D3 stimulate G1 progression and the magnitude of increase we observed for Cyclin D3 in Nup96 heterozygous cells is analogous to that found in various human cancers (Baldassarre et al., 1999; Buschges et al., 1999; Hedberg et al., 2002; Ito et al., 2001). In addition, Cyclin D3 has been shown to be required for lymphocyte development and T cell leukemias (Sicinska et al., 2003). High levels of CDK6 can also accelerate G1 progression (Grossel et al., 1999). Thus, the increased levels of Cyclin D3 and CDK6 observed in Nup96$^{+/-}$ T cells likely contribute to the enhanced proliferation observed in these cells. We detected the mRNA export defects and abnormal protein expression as early as 2 hr after induction of T cell proliferation, when cells were still at their first G1 phase. However, abnormal proliferation of Nup96$^{+/-}$ T cells was only detected after multiple rounds of proliferation, which likely accumulated gene expression defects that contributed to the observed accelerated proliferation of Nup96 mutant cells. We cannot exclude the potential effects of additional genes that were not investigated. Altogether, these results provide evidence that Nup96-mediated regulation of gene expression modulates cell proliferation.

The phase-specific, Nup96-dependent differential regulation of mRNA distribution suggests that Nup96 may interact, directly or indirectly, with selective factors at specific phases of the cell cycle. It is known that different mRNAs can preferentially bind specific subsets of RNA-binding proteins (Kim Guisbert et al., 2005), which may form complexes with specific nucleoporins. Another example of differential export is that of heat shock mRNAs, which are exported by distinct pathways, prior to or following heat shock (Saavedra et al., 1997). To this end, a genome-wide screen was recently performed to identify global and transcript-specific mRNA export pathways in *Drosophila* (Farny et al., 2008). This study showed that unspliced HSP70 transcripts require a smaller number of mRNA export factors than HSP83 transcripts, demonstrating that mRNA export pathways are not identical, as different transcripts associate with specific factors to be exported (Farny et al., 2008). In addition, this study implicated cell cycle regulators in the regulation of

mRNA export. For example, the cyclin-dependent kinase CDK11 was identified as an export factor (Farny et al., 2008) that could potentially regulate the interaction of SR proteins and the mRNA export receptor NXF1 (Hu et al., 2003; Huang et al., 2004). Altogether, these observations point to mechanisms of differential mRNA export.

Nup96 is translated as a Nup98-Nup96 protein precursor containing two nucleoporins (Fontoura et al., 1999), which, by autoproteolysis, yield Nup98 and Nup96 (Rosenblum and Blobel, 1999). Interestingly, the importance of properly regulating the *nup98-nup96* gene is emphasized by the fact that this gene is a target of chromosomal translocations involved in different types of leukemias (Nakamura, 2005). These translocations result in the expression of fusion proteins constituted of the amino-terminal FG repeat region of Nup98 and, variously, the homeodomain transcription factors (Kalverda and Fornerod, 2007). These aberrant proteins transactivate or transrepress target genes, resulting in abnormal gene expression. The fact that the *nup98-nup96* gene is a major target in these leukemias raises the issue that Nup96, which is encoded by the same gene (Fontoura et al., 1999), would also be affected during such translocations. One possibility is that the chromosomal translocations would result in deletion of Nup96 expression in one allele. These cells would likely then express low levels of Nup96. To this end, we show here that low levels of Nup96 enhance cell proliferation. Indeed, abnormal levels of nucleoporins have been reported in many tumors (http://www.oncomine.org/main/index.jsp). Moreover, we have previously shown that Nup96 is upregulated by interferon (Enninga et al., 2002), which is a cytokine known to have antigrowth properties (Gimeno et al., 2005). Since we show here that high levels of Nup96 delay cell cycle progression, it is possible that induction of Nup96 by interferon contributes to the antiproliferative effects of this cytokine. Altogether, these findings underscore the importance of the *nup98-nup96* gene in regulating cell cycle progression. The cell cycle-dependent mRNA distribution and protein expression revealed here add another layer of complexity to the mechanisms controlling cell cycle progression, which are dependent on nucleoporin levels.

EXPERIMENTAL PROCEDURES

Plasmid Construction

Wild-type Nup96 was cloned into myc-pAlter-MAX based on the Nup96 sequence that matches 100% of the human genome sequence (accession AF231130.1), since our original sequence matched 99.7% (accession AF071076). FLAG-Nup96 was generated by PCR and subcloned into the SalI/HindIII sites of pRev TRE (BD Biosciences, San Jose, CA) to generate a tetracycline responsive expression construct. pET28A vectors encoding wild-type UbcH10 and UbcH10:C114-S were provided by R. Basavappa. UbcH10 and UbcH10:C114-S were subcloned into the Sal/Not sites of myc-pAlter-MAX. Ubiquitin (pcDNA3-HA-Ubiquitin) was provided by Z. Nawaz. EGFP-ALADIN was kindly provided by M.J. Matunis.

Cell Culture, Transfections, and Cell Synchronization

293T, HeLa, and NRK cells were grown in DMEM supplemented with 10% FBS and 1% antibiotic-antimycotic (GIBCO, Carlsbad, CA). Transfections were performed with Lipofectamine 2000 (Invitrogen, Carlsbad, CA). HeLa Tet-On cell lines (BD Biosciences) were stably transfected with FLAG-Nup96 and control vector (p-Rev TRE), and maintained in 90% DMEM, 10% FBS (Tet-system approved), 100 μg/ml G418, 1% antibiotic antimycotic, and 300 μg/ml hygromycin B. Cells were induced with 2 μg/ml Doxycyclin for 48 hr. MEF were cultured as described (Jeganathan et al., 2005).

HeLa cell synchronization at the G1/S border was performed with 2 mM thymidine for 15 hr, followed by a 9 hr release in fresh medium, and a second incubation with 2 mM thymidine for 15 hr. Cells in S, early G2, and late G2 phases were collected 4 hr, 7 hr, and 10 hr after release. Mitotic cells were harvested by shake-off in the absence or presence of nocodazole (100 ng/ml), or Taxol (100 nM), or Colcimid (1 μg/ml), 10 hr after the G1/S release. Cells in G2 were collected by harvesting the adherent cells that remained after shaking off mitotic cells. Cells in mid G1 were obtained by culturing mitotic cells in fresh medium for 6 hr. Only adherent cells were collected. Mitotic 293T wells were obtained after treatment with nocodazole (100 ng/μl) for 16 hr. Two millimolar thymidine was added for a period of 16 hr to obtain cells in the G1/S boundary. MEF were synchronized as described (Jeganathan et al., 2005). Measurement of DNA content by flow cytometry was performed to confirm the phases of the cell cycle. For experiments performed with lactacystin, cells were synchronized as above and 10 μM lactacystin was added 3 hr prior to harvesting mitotic cells.

NRK cells were synchronized in S phase with aphidicolin (2.5 ng/ml) for 14 hr. Cells were released and transfected in G2 (5 hr postrelease) with plasmids encoding EGFP alone, myc-Nup96, EGFP-Nup37, or EGFP-ALADIN. Fifty micromolar BrdU was added 11 hr postrelease.

Resting T cells (G0) were selected from spleens, as we described (Faria et al., 2006), using the Dynal Mouse T cell Negative Isolation kit (Invitrogen). T cells were stimulated with 5 ug/ml of anti-CD3 and anti-CD28 antibodies. Two hours poststimulation, T cells were collected in G1 phase. BMDM from 6–8 week old mice were obtained from femur, tibia, and fibula. Cells were then plated at a concentration of 1 million cells/ ml of RPMI containing 15% heat-inactivated FBS and antibiotics. After 24 hr, nonadherent cells were incubated in RPMI containing 4 ng/ml of recombinant mouse macrophage colony stimulating factor (M-CSF) (R&D Systems, Minneapolis, MN). Macrophages were synchronized in G1 in the absence of M-CSF for 18 hr. M-CSF was added back and cells were collected after 16 hr to obtain samples in G2.

Immunoprecipitations and Immunoblots

Immunoprecipitations and immunoblots were performed as described (Faria et al., 2005). The following antibodies were used: Nup107 antibodies were generated against Nup107 (aa 140–699) and were affinity purified; Sec13 antibodies were generated as we described (Enninga et al., 2003); Nup85, Nup37, Nup43, Nup160, Nup153, and Nup62 antibodies were generated as described (Orjalo et al., 2006). hnRNP A1 (a gift from M. Matunis); Cyclin A, Cyclin D3, and Cyclin B1 (Transduction Laboratories, Franklin Lakes, NJ); anti-CD3 and anti-CD28 antibodies (BD Pharmigen, San Diego, CA); anti-actin and anti-FLAG M2 (Sigma, St. Louis, MO); anti-BrdU (BD Biosciences); anti-GFP (Pelletier et al., 2002); anti-myc monoclonal antibody (Roche); anti-myc polyclonal antibody (Santa Cruz Biotechnology, Santa Cruz, CA); anti-HA 12CA5 (Roche, Palo Alto, CA); anti-CDK6 (Santa Cruz Biotechnology); IκBα (Abcam, Cambridge, MA). Immunoblots were quantified using the ImageJ program. Sucrose gradient sedimentation was performed as described (Loiodice et al., 2004).

BrdU Staining, Immunofluorescence, and Microscopy

For BrdU staining, cells were washed, fixed with 4% formaldehyde (EM grade-Polysciences, Warrington, PA) for 30 min, and permeabilized with acetone at −20°C for 5 min. Cells were washed in PBS, permeabilized with 2N HCl for 10 min, blocked with PBS/1% BSA/0.1% TWEEN-20 for 5 min, and incubated with anti-myc antibodies (to detect Nup96) or anti-GFP antibodies (to amplify the GFP signal), and anti-BrdU antibody for 25 min at 37°C. Cells were incubated with secondary antibodies, washed, and DAPI was added. Samples were analyzed by Apotome microscopy in a Zeiss Axiovert 200M (Thornwood, NY). Live cell imaging was performed as previously described (Jeganathan et al., 2005).

In Situ Hybridization and Flow Cytometry

For the in situ hybridization procedures, HeLa cells were washed, fixed in formaldehyde for 10 min, and permeabilized in 70% ethanol overnight, at −20°C. Cells were then treated with 10% DEPC in ethanol for 1 hr, centrifuged at 12,000 × g for 20 s, and then resuspended in 0.5% Tween in PBS. Cells were subjected to oligo-dT in situ hybridization as described (Chakraborty

et al., 2006), washed, stained with propidium iodide, and subjected to flow cytometry.

Oligo-dT in situ hybridization or in situ hybridization performed with specific probes were carried out as we described (Chakraborty et al., 2006). Samples were analyzed by Apotome microscopy. Quantification of image intensities was performed using the Axiovision 4.0 image analysis software.

For flow cytometry procedures, T cells were washed in PBS and fixed with ice cold 70% ethanol for 18 hr at 4°C. Cells were then stained with a mixture of PI/RNase solution in PBS and resuspended at 1 million cells per ml for FACS analysis. Cells at different phases of the cell cycle were analyzed using the Cell Quest software.

T Cell and Macrophage Proliferation Assays

T cells were obtained from spleens of Nup96$^{+/+}$ and Nup96$^{+/-}$ mice and labeled with 5 μM CSFE (Molecular Probes, Carlsbad, CA) in RPMI for 15 min at 37°C. Cells were washed with RPMI containing 2% FBS and plated in RPMI containing 10% FBS. T cell proliferation was induced by anti-CD3 and anti-CD28 antibodies at 5 μg/ml. Samples were collected at 0, 24, and 48 hr. CSFE intensity was analyzed by flow cytometry.

BMDM were maintained in culture for 7 d. M-CSF containing medium was replenished at day 3 and day 7 of culture. Experiments were then performed between day 8 and day 12. The macrophage proliferation assay was carried out with ~30,000 cells per well in RPMI medium containing 4 ng/ml M-CSF alone or 10% WEHI medium (IL-3 conditioned) and 20% MEF-conditioned medium (R&D Systems). Proliferation was assessed on days 2, 3, and 4, using the CellTiter 96® Non-Radioactive Cell Proliferation Assay kit (Promega, Madison, WI).

Cell Fractionation and Real-Time PCR Analysis

Cell fractionation, RNA isolation, and RT-PCR were performed as described (Wang et al., 2006).

SUPPLEMENTAL DATA

Supplemental Data include two figures and can be with this article online at http://www.developmentalcell.com/cgi/content/full/15/5/657/DC1/.

ACKNOWLEDGMENTS

We thank A. Levay, D.R. Nussenzveig, and K. Jeganathan for assistance. We thank R. Basavappa, Z. Nawaz, and M. Matunis for reagents. This work was supported by NIH R01AI28900 and U54AI5715801 to D.E.L., and R01 GM07159-01 to B.M.A.F.

Received: September 16, 2007
Revised: July 13, 2008
Accepted: August 28, 2008
Published: November 10, 2008

REFERENCES

Aitchison, J.D., Blobel, G., and Rout, M.P. (1995). Nup120p: a yeast nucleoporin required for NPC distribution and mRNA transport. J. Cell Biol. *131*, 1659–1675.

Baldassarre, G., Belletti, B., Bruni, P., Boccia, A., Trapasso, F., Pentimalli, F., Barone, M.V., Chiappetta, G., Vento, M.T., Spiezia, S., et al. (1999). Overexpressed cyclin D3 contributes to retaining the growth inhibitor p27 in the cytoplasm of thyroid tumor cells. J. Clin. Invest. *104*, 865–874.

Ball, J.R., Dimaano, C., Bilak, A., Kurchan, E., Zundel, M.T., and Ullman, K.S. (2007). Sequence preference in RNA recognition by the nucleoporin Nup153. J. Biol. Chem. *282*, 8734–8740.

Belgareh, N., Rabut, G., Bai, S.W., van Overbeek, M., Beaudouin, J., Daigle, N., Zatsepina, O.V., Pasteau, F., Labas, V., Fromont-Racine, M., et al. (2001). An evolutionary conserved NPC subcomplex, which redistributes in part to kinetochores in mammalian cells. J. Cell Biol. *154*, 1147–1160.

Boehmer, T., Enninga, J., Dales, S., Blobel, G., and Zhong, H. (2003). Depletion of a single nucleoporin, Nup107, prevents the assembly of a subset of nucleoporins into the nuclear pore complex. Proc. Natl. Acad. Sci. USA *100*, 981–985.

Boehmer, T., Blobel, G., and Glavy, J.S. (2004). Members of the Nup107–160 subcomplex are phosphorylated in mitosis. ASCB 44th Annual Meeting Abstract 1807, 472a.

Buschges, R., Weber, R.G., Actor, B., Lichter, P., Collins, V.P., and Reifenberger, G. (1999). Amplification and expression of cyclin D genes (CCND1, CCND2 and CCND3) in human malignant gliomas. Brain Pathol. *9*, 435–442.

Chakraborty, P., Satterly, N., and Fontoura, B.M. (2006). Nuclear export assays for poly(A) RNAs. Methods *39*, 363–369.

D'Angelo, M.A., Anderson, D.J., Richard, E., and Hetzer, M.W. (2006). Nuclear pores form de novo from both sides of the nuclear envelope. Science *312*, 440–443.

Dockendorff, T.C., Heath, C.V., Goldstein, A.L., Snay, C.A., and Cole, C.N. (1997). C-terminal truncations of the yeast nucleoporin Nup145p produce a rapid temperature-conditional mRNA export defect and alterations to nuclear structure. Mol. Cell. Biol. *17*, 906–920.

Emtage, J.L., Bucci, M., Watkins, J.L., and Wente, S.R. (1997). Defining the essential functional regions of the nucleoporin Nup145p. J. Cell Sci. *110*, 911–925.

Enninga, J., Levy, D.E., Blobel, G., and Fontoura, B.M. (2002). Role of nucleoporin induction in releasing an mRNA nuclear export block. Science *295*, 1523–1525.

Enninga, J., Levay, A., and Fontoura, B.M. (2003). Sec13 shuttles between the nucleus and the cytoplasm and stably interacts with Nup96 at the nuclear pore complex. Mol. Cell. Biol. *23*, 7271–7284.

Faria, P.A., Chakraborty, P., Levay, A., Barber, G.N., Ezelle, H.J., Enninga, J., Arana, C., van Deursen, J., and Fontoura, B.M. (2005). VSV disrupts the Rae1/mrnp41 mRNA nuclear export pathway. Mol. Cell *17*, 93–102.

Faria, A.M., Levay, A., Wang, Y., Kamphorst, A.O., Rosa, M.L., Nussenzveig, D.R., Balkan, W., Chook, Y.M., Levy, D.E., and Fontoura, B.M. (2006). The nucleoporin Nup96 is required for proper expression of interferon-regulated proteins and functions. Immunity *24*, 295–304.

Farny, N.G., Hurt, J.A., and Silver, P.A. (2008). Definition of global and transcript-specific mRNA export pathways in metazoans. Genes Dev. *22*, 66–78.

Fontoura, B.M., Blobel, G., and Matunis, M.J. (1999). A conserved biogenesis pathway for nucleoporins: proteolytic processing of a 186-kilodalton precursor generates nup98 and the novel nucleoporin, nup96. J. Cell Biol. *144*, 1097–1112.

Franz, C., Walczak, R., Yavuz, S., Santarella, R., Gentzel, M., Askjaer, P., Galy, V., Hetzer, M., Mattaj, I.W., and Antonin, W. (2007). MEL-28/ELYS is required for the recruitment of nucleoporins to chromatin and postmitotic nuclear pore complex assembly. EMBO Rep. *8*, 165–172.

Gimeno, R., Lee, C.K., Schindler, C., and Levy, D.E. (2005). Stat1 and Stat2 but not Stat3 arbitrate contradictory growth signals elicited by α/β interferon in T lymphocytes. Mol. Cell. Biol. *25*, 5456–5465.

Grossel, M.J., Baker, G.L., and Hinds, P.W. (1999). cdk6 can shorten G(1) phase dependent upon the N-terminal INK4 interaction domain. J. Biol. Chem. *274*, 29960–29967.

Harel, A., and Forbes, D.J. (2004). Importin beta: conducting a much larger cellular symphony. Mol. Cell *16*, 319–330.

Harel, A., Orjalo, A.V., Vincent, T., Lachish-Zalait, A., Vasu, S., Shah, S., Zimmerman, E., Elbaum, M., and Forbes, D.J. (2003). Removal of a single pore subcomplex results in vertebrate nuclei devoid of nuclear pores. Mol. Cell *11*, 853–864.

Hedberg, Y., Roos, G., Ljungberg, B., and Landberg, G. (2002). Cyclin D3 protein content in human renal cell carcinoma in relation to cyclin D1 and clinicopathological parameters. Acta Oncol. *41*, 175–181.

Hoffmann, A., Levchenko, A., Scott, M.L., and Baltimore, D. (2002). The IκB-NF-κB signaling module: temporal control and selective gene activation. Science *298*, 1241–1245.

Hu, D., Mayeda, A., Trembley, J.H., Lahti, J.M., and Kidd, V.J. (2003). CDK11 complexes promote pre-mRNA splicing. J. Biol. Chem. *278*, 8623–8629.

Huang, Y., Yario, T.A., and Steitz, J.A. (2004). A molecular link between SR protein dephosphorylation and mRNA export. Proc. Natl. Acad. Sci. USA *101*, 9666–9670.

Ito, Y., Takeda, T., Wakasa, K., Tsujimoto, M., and Matsuura, N. (2001). Expression and possible role of cyclin D3 in human pancreatic adenocarcinoma. Anticancer Res. *21*, 1043–1048.

Jeganathan, K.B., Malureanu, L., and van Deursen, J.M. (2005). The Rae1-Nup98 complex prevents aneuploidy by inhibiting securin degradation. Nature *438*, 1036–1039.

Kalverda, B., and Fornerod, M. (2007). The nuclear life of nucleoporins. Dev. Cell *13*, 164–165.

Kim Guisbert, K., Duncan, K., Li, H., and Guthrie, C. (2005). Functional specificity of shuttling hnRNPs revealed by genome-wide analysis of their RNA binding profiles. RNA *11*, 383–393.

Loiodice, I., Alves, A., Rabut, G., Van Overbeek, M., Ellenberg, J., Sibarita, J.B., and Doye, V. (2004). The entire Nup107–160 complex, including three new members, is targeted as one entity to kinetochores in mitosis. Mol. Biol. Cell *15*, 3333–3344.

Makhnevych, T., Lusk, C.P., Anderson, A.M., Aitchison, J.D., and Wozniak, R.W. (2003). Cell cycle regulated transport controlled by alterations in the nuclear pore complex. Cell *115*, 813–823.

Maul, G.G., Maul, H.M., Scogna, J.E., Lieberman, M.W., Stein, G.S., Hsu, B.Y., and Borun, T.W. (1972). Time sequence of nuclear pore formation in phytohemagglutinin-stimulated lymphocytes and in HeLa cells during the cell cycle. J. Cell Biol. *55*, 433–447.

Maul, G.G., Deaven, L.L., Freed, J.J., Campbell, G.L., and Becak, W. (1980). Investigation of the determinants of nuclear pore number. Cytogenet. Cell Genet. *26*, 175–190.

Murray, A.W. (2004). Recycling the cell cycle: cyclins revisited. Cell *116*, 221–234.

Nakamura, T. (2005). NUP98 fusion in human leukemia: dysregulation of the nuclear pore and homeodomain proteins. Int. J. Hematol. *82*, 21–27.

Orjalo, A.V., Arnaoutov, A., Shen, Z., Boyarchuk, Y., Zeitlin, S.G., Fontoura, B., Briggs, S., Dasso, M., and Forbes, D.J. (2006). The Nup107–160 nucleoporin complex is required for correct bipolar spindle assembly. Mol. Biol. Cell *17*, 3806–3818.

Pelletier, L., Stern, C.A., Pypaert, M., Sheff, D., Ngo, H.M., Roper, N., He, C.Y., Hu, K., Toomre, D., Coppens, I., et al. (2002). Golgi biogenesis in *Toxoplasma gondii*. Nature *418*, 548–552.

Peters, J.M. (2002). The anaphase-promoting complex: proteolysis in mitosis and beyond. Mol. Cell *9*, 931–943.

Rasala, B.A., Orjalo, A.V., Shen, Z., Briggs, S., and Forbes, D.J. (2006). ELYS is a dual nucleoporin/kinetochore protein required for nuclear pore assembly and proper cell division. Proc. Natl. Acad. Sci. USA *103*, 17801–17806.

Rosenblum, J.S., and Blobel, G. (1999). Autoproteolysis in nucleoporin biogenesis. Proc. Natl. Acad. Sci. USA *96*, 11370–11375.

Saavedra, C.A., Hammell, C.M., Heath, C.V., and Cole, C.N. (1997). Yeast heat shock mRNAs are exported through a distinct pathway defined by Rip1p. Genes Dev. *11*, 2845–2856.

Sicinska, E., Aifantis, I., Le Cam, L., Swat, W., Borowski, C., Yu, Q., Ferrando, A.A., Levin, S.D., Geng, Y., von Boehmer, H., et al. (2003). Requirement for cyclin D3 in lymphocyte development and T cell leukemias. Cancer Cell *4*, 451–461.

Teixeira, M.T., Siniossoglou, S., Podtelejnikov, S., Benichou, J.C., Mann, M., Dujon, B., Hurt, E., and Fabre, E. (1997). Two functionally distinct domains generated by in vivo cleavage of Nup145p: a novel biogenesis pathway for nucleoporins. EMBO J. *16*, 5086–5097.

Townsley, F.M., Aristarkhov, A., Beck, S., Hershko, A., and Ruderman, J.V. (1997). Dominant-negative cyclin-selective ubiquitin carrier protein E2-C/UbcH10 blocks cells in metaphase. Proc. Natl. Acad. Sci. USA *94*, 2362–2367.

Tran, E.J., and Wente, S.R. (2006). Dynamic nuclear pore complexes: life on the edge. Cell *125*, 1041–1053.

van Stipdonk, M.J., Lemmens, E.E., and Schoenberger, S.P. (2001). Naive CTLs require a single brief period of antigenic stimulation for clonal expansion and differentiation. Nat. Immunol. *2*, 423–429.

Vasu, S., Shah, S., Orjalo, A., Park, M., Fischer, W.H., and Forbes, D.J. (2001). Novel vertebrate nucleoporins Nup133 and Nup160 play a role in mRNA export. J. Cell Biol. *155*, 339–353.

Walther, T.C., Alves, A., Pickergill, H., Loiodice, I., Hetzer, M., Galy, V., Hulsmann, B.B., Kocher, T., Wilm, M., Allen, T., et al. (2003). The conserved Nup107–160 complex is critical for nuclear pore complex assembly. Cell *113*, 195–206.

Wang, Y., Zhu, W., and Levy, D.E. (2006). Nuclear and cytoplasmic mRNA quantification by SYBR green based real-time RT-PCR. Methods *39*, 356–362.

Whitfield, M.L., Sherlock, G., Saldanha, A.J., Murray, J.I., Ball, C.A., Alexander, K.E., Matese, J.C., Perou, C.M., Hurt, M.M., Brown, P.O., et al. (2002). Identification of genes periodically expressed in the human cell cycle and their expression in tumors. Mol. Biol. Cell *13*, 1977–2000.

Winey, M., Yarar, D., Giddings, T.H., Jr., and Mastronarde, D.N. (1997). Nuclear pore complex number and distribution throughout the *Saccharomyces cerevisiae* cell cycle by three-dimensional reconstruction from electron micrographs of nuclear envelopes. Mol. Biol. Cell *8*, 2119–2132.

Zuccolo, M., Alves, A., Galy, V., Bolhy, S., Formstecher, E., Racine, V., Sibarita, J.B., Fukagawa, T., Shiekhattar, R., Yen, T., et al. (2007). The human Nup107–160 nuclear pore subcomplex contributes to proper kinetochore functions. EMBO J. *26*, 1853–1864.